Catal Lett (2017) 147:1722–1731
DOI 10.1007/s10562-017-2066-9

Preparative Aspects of Supported Ni_2P Catalysts for Reductive Upgrading of Technical Lignin to Aromatics

Tamás I. Korányi[1] · Emiel J. M. Hensen[1]

Received: 26 March 2017 / Accepted: 18 April 2017 / Published online: 26 May 2017

Abstract Supported Ni_2P was evaluated as a hydrodeoxygenation (HDO) catalyst in the reductive upgrading of a soda lignin in supercritical ethanol by a hydrotalcite-derived mixed Cu-Mg-Al oxide ($CuMgAlO_x$) catalyst. Various Ni_2P catalysts were prepared by different approaches on silica, γ-alumina and a siliceous amorphous silica-alumina (ASA) supports. Calcined NiO/SiO_2 precursors were impregnated with phosphate, phosphite and hypophosphite followed by reduction. With γ-alumina, the desired Ni_2P could not be obtained, presumably due to the reaction of the P-source with alumina. NiO on ASA could be converted to Ni_2P by addition of phosphite, preferably at a P/Ni ratio of 1. Low P/Ni ratio avoids blockage of the pores by P-oxide species remaining after reduction. By further comparison to a sol–gel prepared NiO/SiO_2 and co-impregnated silica, it was established that the most active Ni_2P catalyst was obtained by impregnation of NiO/SiO_2 with phosphate at P/Ni = 1 and reduction at 620 °C. In combination with $CuMgAlO_x$, more than half of soda lignin can be converted to aromatics monomers with a relatively high degree of deoxygenation and limited degree of ring hydrogenation. The co-catalyst system is more active than the separate catalysts.

Graphical Abstract

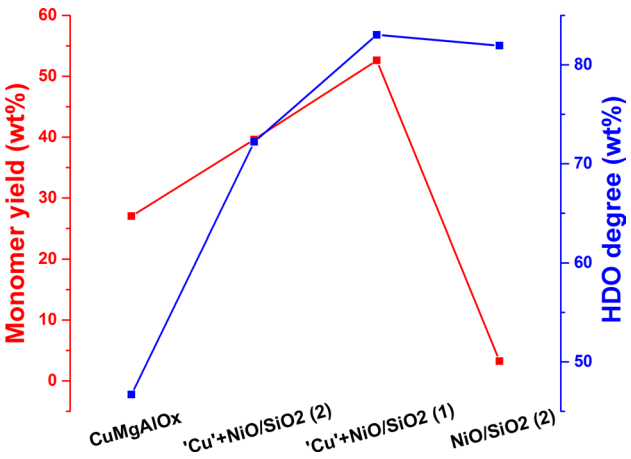

Keywords Hydrodeoxygenation · Nickel phosphide · Silica · Lignin · Aromatics

1 Introduction

Lignin is the second most abundant biopolymer on Earth after cellulose, comprising 15–30% of the dry weight and approximately 40% of the energy content of land-based plant biomass [1, 2]. Lignin is a complex three-dimensional amorphous polymer consisting of methoxylated phenylpropane structures [3, 4]. It is nature's largest reserve of aromatics, yet mostly burned as low-grade boiler fuel for energy recovery in the paper and pulping industry [3, 5]. Catalytic upgrading of lignin is regarded as a promising approach to add more value to this side-stream of biorefineries [1–6]. In recent years, a large number of such approaches have been explored using different types of

Electronic supplementary material The online version of this article (doi:10.1007/s10562-017-2066-9) contains supplementary material, which is available to authorized users.

✉ Emiel J. M. Hensen
e.j.m.hensen@tue.nl

[1] Schuit Institute of Catalysis, Inorganic Materials Chemistry, Eindhoven University of Technology, P.O. Box 513, 5600 MB Eindhoven, The Netherlands

catalytic chemistry. Most of this work has been covered in several reviews [1–7]. Amongst others, catalytic hydrogenation (HYD) is often used to upgrade lignin or the products derived from lignin depolymerization. Aromatics (BTX) and alkylphenols are usually targeted by such methods, because they are valuable platform molecules in the chemical industry [1].

The promise of using alcohol solvents for lignin depolymerization has already been early recognized [8–10]. Homogeneous Lewis acid catalysts facilitate the deconstruction of lignin in alcohols at relatively high temperature [11]. Recent studies by Güvenatam et al. demonstrate that soda lignin can be effectively converted in a mixture of hydrocarbon products both in ethanol and ethanol/water mixtures [12]. Barta et al. used a heterogeneous Cu-doped porous metal oxide catalyst (Cu-PMO) obtained by calcination of a hydrotalcite precursor to depolymerize lignin in supercritical methanol [13, 14]. This catalyst also displayed activity in the partial removal of oxygen from the products. Under relatively harsh conditions (300 °C, ~200 bar autogenous pressure) not only lignin but also lignocellulosic biomass such as wood chips could be nearly completely converted into useful chemicals [15]. Huang et al. found that carrying out a similar lignin depolymerization process in ethanol instead of methanol using a Cu–Mg–Al mixed oxide catalyst resulted in higher aromatics yield and less char by-product [8–10]. The better performance in ethanol is in keeping with an earlier report by Cheng et al. [16].

The group of Ford concluded that reaction in methanol leads to nearly complete hydrogenation of the aromatic rings [13, 17]. This would be unattractive from the economic point of view as hydrogen is too costly [18]. The conclusion of Barta et al. that all aromatic rings were hydrogenated is based on the erroneous interpretation of HSQC NMR data, which showed the disappearance of aromatic C–H groups in the products. The alternative interpretation is that the aromatic rings were extensively alkylated by methanol. This was confirmed in the work of Huang et al. [9]. Overall, the aromatic monomers yields are higher when depolymerization of lignin is carried out in ethanol than in methanol [16, 19, 20]. Ethanol has several functions: it dissolves lignin, it chemically protects the useful lignin fragments against undesired repolymerization by alkylation of aromatic rings and phenolic groups and it is a source of hydrogen to facilitate the hydrogenative removal of oxygen functionalities from the fragments [8]. Ethanol also acts as formaldehyde scavenger, which is involved in reactions of lignin fragments to higher molecular-weight products [9].

Transition metal phosphides constitute a promising class of hydrotreating catalysts, because they do not require sulfidation, their preparation is relatively easy, they do not contain noble metals, and they are able to activate hydrogen [21]. Metal phosphides are usually prepared by simultaneous reduction of a metal salt or oxide and a phosphorus compound with hydrogen [22]. In the classical phosphate method, the catalyst support is loaded with a metal nitrate and ammonium phosphate, followed by reduction at elevated temperature (500–800 °C). Alternative sources of phosphorus such as phosphite, hypophosphite, and phosphine require lower reduction temperatures, which is beneficial as higher dispersion of the final metal phosphide phase is possible [22]. Most frequently silica is used as catalyst support, but alumina was also evaluated in some special cases [23, 24].

Aside from application as a catalyst for hydrodesulfurization (HDS) [25, 26], Ni_2P/SiO_2 has also been used as a hydrodeoxygenation (HDO) catalyst for upgrading of bio-oil obtained by pyrolysis of lignocellulosic biomass [27]. Ni/SiO_2 has also been employed to depolymerize lignin in the presence of molecular hydrogen, mainly yielding substituted alicyclic and aromatic hydrocarbons [28]. The use of Ni-phosphide catalysts instead of reduced Ni is explored in this work in order to retain high HDO reaction rate and to lower the rate of aromatic ring hydrogenation. The use of Ni-phosphide catalysts in combination with $CuMgAlO_x$ is explored here, as the latter catalyst generates hydrogen during ethanolysis of lignin [10]. This hydrogen is used to activate reduced and passivated Ni_2P/SiO_2 [22] and for the HDO reactions. We also paid attention to the conversion of ethanol, as solvent usage should be limited in practice.

In this work, we optimized the preparation of nickel phosphide catalysts towards the HDO of lignin oil and technical lignin. The conversion of technical lignin was done in a two-catalyst system involving supported Ni-phosphide and the earlier described $CuMgAlO_x$ catalyst. We varied the P precursor and the reduction temperature for silica, amorphous silica alumina (ASA) and alumina supported catalysts. We also explored alternative preparation methods on silica and carbon supports. From this work, the optimal catalyst appeared to be a Ni_2P/SiO_2 catalyst prepared using phosphate as the precursor. In combination with $CuMgAlO_x$, the catalyst is able to obtain a yield of aromatic monomers of 53 wt% at a high HDO degree of 83 wt%.

2 Experimental Methods

2.1 Chemicals and Materials

Protobind 1000 alkali lignin was purchased from GreenValue. This lignin was obtained by soda pulping of wheat straw (sulfur-free lignin with less than 4 wt% carbohydrates and less than 2 wt% ash). All commercial chemicals

were analytical reagents and were used without further purification.

2.2 Catalyst Preparation

For the Ni-containing catalysts the metal loading was fixed at 10 wt%. Commercial silica (SiO_2) and alumina (γ-Al_2O_3, Ketjen CK300) supports were used and are denoted as SiO_2 and Al_2O_3, respectively. Amorphous silica alumina, denoted as ASA and nominally composed of 5 wt% Al_2O_3 and 95 wt% SiO_2, was prepared by alumination of silica at pH 9 followed by calcination at 500 °C [29]. All supports were sieved to 125–250 µm size before further use.

The catalysts prepared in this study are listed in Table 1. Silica-supported catalysts were prepared with P/Ni atomic ratios equal to or higher than two (entries 1–5 in Table 1). The dried silica supports were impregnated with aqueous solutions of $Ni(NO_3)_2{\cdot}6H_2O$. The impregnated catalysts were dried overnight in air at 110 °C, and then calcined at 550 °C for 5 h. These NiO/SiO_2 catalysts were impregnated with aqueous solutions of $(NH_4)_2HPO_4$ (P/Ni = 2), H_3PO_3 (P/Ni = 2 or 6), or H_3PO_2 (P/Ni = 2), dried overnight in air at 100 °C, and then reduced in 100 ml/min H_2 flow at varying temperatures for 3 h after heating at 1 °C/min. The resulting catalysts were designated as NiO/SiO_2(*r*, PO_x) in which *r* is the P/Ni ratio and PO_x the phosphorus oxide precursor (PO_4^{3-}, PO_3^{3-} or PO_2^{3-}). In this way, we prepared NiO/SiO_2 (2, PO_4), NiO/SiO_2 (2, PO_3), NiO/SiO_2 (2, PO_2) and NiO/SiO_2 (6, PO_3) (entries 1–4 in Table 1). The reduced catalysts were cooled to room temperature in hydrogen, and passivated in 100 ml/min 1% O_2 containing N_2 gas mixture.

Another catalyst was prepared by a modified sol–gel (SG) procedure [30]: 7.52 g $Ni(NO_3)_2{\cdot}6H_2O$ and 5.42 g urea were dissolved in 295 ml water and its pH was adjusted to 2.3 by concentrated HNO_3. An amount of 32 ml TEOS and 29 ml ethanol were mixed and filled into a 100 ml dropping funnel. This solution was added dropwise into the stirred $Ni(NO_3)_2$-urea solution. During continuous stirring the temperature and the pH were increased to 80 °C and 5.7, respectively, resulting in a dark green gel. After 10 h stirring, the mixture was cooled to room temperature, filtered, and washed with ethanol and water. The dried and sieved precursor was calcined at 550 °C for 5 h, then impregnated with H_3PO_3 (P/Ni = 2) and finally reduced at 540 °C for 3 h. This catalyst is designated as NiO/SiO_2-SG (2, PO_3) (entry 5 in Table 1).

In order to study the effect of the support and initial P/Ni ratios ASA and Al_2O_3 supported catalysts were prepared at P/Ni ratios of 1 and 4, resulting in NiO/Al_2O_3 (4, PO_3), NiO/Al_2O_3 (1, PO_2), NiO/ASA (4, PO_3) and NiO/ASA (1, PO_3) (entries 6–9 in Table 1). The preparation procedure was the same as described above and calcination and reduction were done at 550 and 540 °C, respectively, with the exception of the hypophosphite (H_3PO_2) precursor for which a reduction temperature of 400 °C was used (entry 9 in Table 1).

The mode of impregnation was studied in this series on sol–gel prepared NiO/silica (NiO/SiO_2-SG) and commercial silica (SiO_2) supports using a P/Ni ratio of 1 (entries 10–14 in Table 1). NiO/SiO_2-SG (1, PO_4) and NiO/SiO_2-SG (1, PO_3) were prepared by impregnating the P precursor to the calcined sol–gel prepared NiO/SiO_2 precursor. Co-impregnation of silica with combinations of $Ni(NO_3)_2$ with either $(NH_4)_2HPO_4$ or H_3PO_3 led to Ni/SiO_2 (1, PO_4) and Ni/SiO_2 (1, PO_3). These catalysts were not calcined prior to reduction. Another catalyst was consecutively impregnated NiO/SiO_2 (1, PO_4). Phosphate and phosphite precursors were reduced at 620 and 540 °C, respectively.

Table 1 Preparation method of Ni-based catalysts, initial P/Ni ratio, reduction temperature and phase analysis by XRD

Entry	Catalyst	Mode of impregnation	$(P/Ni)_{initial}$	T_{red} (°C)	$Phase_{XRD}$
1	NiO/SiO_2 (2, PO_4)	Consecutive	2	620	Ni_2P
2	NiO/SiO_2 (2, PO_3)	Consecutive	2	540	Ni_2P
3	NiO/SiO_2 (6, PO_3)	Consecutive	6	400	Phosphates + Ni_5P_2
4	NiO/SiO_2 (2, PO_2)	Consecutive	2	400	Ni_2P
5	NiO/SiO_2-SG (2, PO_3)	Sol–gel, consecutive	2.57	540	Ni_2P
6	NiO/ASA (4, PO_3)	Consecutive	4.43	540	$Ni_2P + Al(OH)_3 + SiO_2$
7	NiO/ASA (1, PO_3)	Consecutive	1	540	Ni_2P
8	NiO/Al_2O_3 (4, PO_3)	Consecutive	4.02	540	Al_2O_3
9	NiO/Al_2O_3 (1, PO_2)	Consecutive	1	400	Al_2O_3
10	NiO/SiO_2-SG (1, PO_4)	Sol–gel, consecutive	1	620	Ni_2P
11	NiO/SiO_2-SG (1, PO_3)	Sol–gel, consecutive	1	540	Ni_2P
12	Ni/SiO_2 (1, PO_4)	Co-impregnation	1	620	Ni_2P
13	Ni/SiO_2 (1, PO_3)	Co-impregnation	1	540	Ni_2P
14	NiO/SiO_2 (1, PO_4)	Consecutive	1	620	Ni_2P

A detailed recipe for the preparation of the 20 wt% Cu containing $CuMgAlO_x$ catalysts with (Cu + Mg)/Al = 2 molar ratio is given elsewhere [8]. Briefly, $Cu(NO_3)_2$, $Mg(NO_3)_2$, and $Al(NO_3)_3$ salts were dissolved in water. This solution, along with a NaOH solution, was added dropwise to a Na_2CO_3 solution at 60 °C with stirring, whilst keeping the pH at 10. The slurry was aged at 60 °C under stirring for 24 h. The precipitate was filtered, washed, and dried. The hydrotalcite-like precursor was calcined at 460 °C for 6 h in air.

2.3 Catalyst Characterization

H_2-TPR of catalyst precursors was conducted on a Micromeritics Autochem II chemisorption analyzer. An amount of 50 mg catalyst precursor was loaded into a quartz U-tube reactor. The reduction was performed with a 4 vol% H_2/N_2 flow (50 ml/min) at a rate of 1 °C /min. The H_2 consumption was determined using a thermal conductivity detector (TCD).

Elemental analysis was done by inductively coupled plasma optical emission spectroscopy (ICP-OES) on a Spectro CIROS CCD spectrometer equipped with a free-running 27.12 MHz generator at 1400 W. Samples were dissolved in an equivolumetric mixture of aqueous solutions of 40% HF, 65% HNO_3 and water.

Powder X-ray diffraction (XRD) was measured on a Bruker Endeavor D2 with Cu Kα radiation (40 kV and 30 mA). Patterns were recorded with 0.02° steps over the 10°–85° angular range with 1 s counting time per step.

N_2 physisorption was measured on a Tristar 3000 system. The samples were degassed at 300 °C for 5 h prior to measurements. The surface areas were determined by the Brunauer–Emmett–Teller (BET) equation. The pore volumes and average pore diameters were determined by the Barrett–Joyner–Halenda (BJH) method from the desorption branches of the isotherms.

2.4 Catalytic Activity Measurements

Lignin conversion experiments were carried out in two types of stainless-steel high-pressure autoclaves (50 ml AmAr or 100 ml Parr). Typically, the autoclave was charged with a suspension of 0.2 or 0.5 g catalyst and 0.4 or 1.0 g lignin in 20 or 40 ml ethanol, respectively. When two catalysts were combined, the autoclave was charged with 0.2 (0.5) g $CuMgAlO_x$ and 0.2 (0.5) g Ni-containing catalysts. The reactor was sealed and purged with nitrogen several times to remove oxygen. After leak testing, the pressure was increased to 20 bar with nitrogen or with hydrogen and the reaction mixture was heated to 340 °C under continuous stirring at 500 rpm within 1 h. After the reaction, the heating oven was removed, and the reactor was allowed to cool to room temperature. The liquid phase product mixture was analyzed by a Shimadzu 2010 GC-MS system equipped with a RTX-1701 column (60 m × 0.25 mm × 0.25 μm) and a flame ionization detector (FID) together with a mass spectrometer (MS) detector. Identification of products was based on a search of the MS spectra with the NIST11 and NIST11s MS libraries. The GC peaks with the same molecular weight (Mw) were unified and presented by the structure determined by GC-MS. These products were further divided into four groups, namely hydrogenated cyclics (−O (oxygen-free)) [HC^{-O}], hydrogenated cyclics (+O (oxygen-containing)) [HC^{+O}], aromatics (−O) [Ar^{-O}] and aromatics (+O) [Ar^{+O}], according to the nature of the ring structure and functional groups. The FID response factors were calculated using the Effective Carbon Number (ECN) method [31] relative to n-dodecane, which served as the internal standard. The lignin monomers and ethanol product yields, the aromatic hydrogenation (HYD) and hydrodeoxygenation (HDO) degrees were determined using Eqs. (1–4):

$$\text{Lignin monomers yield (wt\%)} = (\text{weight of monomers})/(\text{weight of starting lignin}) \times 100 \quad (1)$$

$$\text{Ethanol product yield (wt\%)} = (\text{weight of EtOH products})/(\text{weight of starting EtOH}) \times 100 \quad (2)$$

$$\text{Aromatic HYD degree (wt\%)} = \left(HC^{-O} + HC^{+O}\right)/(\text{Lignin yield}) \times 100 \quad (3)$$

$$\text{HDO degree (wt\%)} = \left(HC^{-O} + Ar^{-O}\right)/(\text{Lignin yield}) \times 100 \quad (4)$$

3 Results and Discussion

3.1 Silica-Supported Catalysts with P/Ni ≥ 2

Five silica-supported nickel phosphide catalysts were prepared at a P/Ni precursor ratio equal to or higher than 2 (Table 1, entries 1–5). A higher than stoichiometric precursor ratio was initially chosen, because it is known that excess phosphorus is needed to obtain Ni_2P [22, 32]. Ni_2P is usually the preferred nickel phosphide phase, for instance when guaiacol is being deoxygenated [33]. An initial P/Ni of 2 ratio was determined to be optimum for preparing active Ni_2P/SiO_2 catalysts for guaiacol HDO, in line with the optimum preparation for HDS reactions [34]. According to a detailed XRD studh, the reduction proceeds through formation of metallic Ni at about

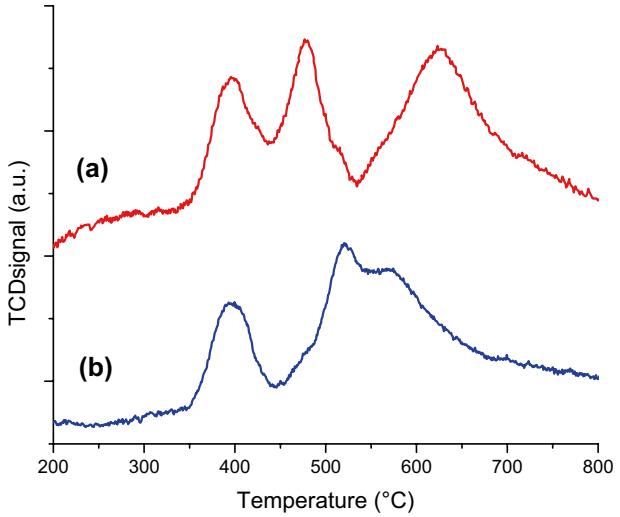

Fig. 1 TPR curve (1 °C/min–800 °C) of consecutively impregnated *a* $NiO/SiO_2 + (NH_4)_2HPO_4$ precursor (later NiO/SiO_2 (2, PO_4) catalyst) and *b* $NiO/SiO_2 + H_3PO_3$ precursor (later NiO/SiO_2 (2, PO_3) catalyst)

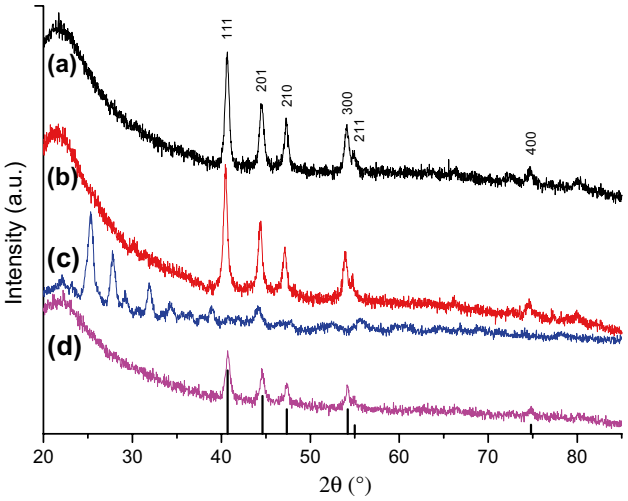

Fig. 2 XRD patterns of *a* NiO/SiO_2 (2, PO_4), *b* NiO/SiO_2 (2, PO_3), *c* NiO/SiO_2 (6, PO_3), and *d* NiO/SiO_2 (2, PO_2) catalysts. *Reference lines* of Ni_2P are marked at the *bottom*

400 °C followed by formation of Ni_2P at about 550 °C when the P precursor is reduced [35]. TPR is typically employed to determine the lowest reduction temperature that lead to Ni_2P. The TPR traces for NiO/SiO_2 (2, PO_4) and NiO/SiO_2 (2, PO_3) show reduction features at 398, 478, 624, 732 °C (Fig. 1a) and 395, 478, 517, 565 °C (Fig. 1b), respectively. Based on literature [33, 35, 36], we can assign the first two reduction features to formation of metallic Ni and the latter two to the reduction of the phosphorus oxides precursors. Accordingly, we selected 620 and 540 °C as reduction temperatures for the phosphate and phosphite containing catalysts. The relative peak areas derived from TPR determined for Ni (former two peaks) and P (latter two peaks) reduction are 1.00 and 1.05 for NiO/SiO_2 (2, PO_4) and 0.95 and 2.91 for NiO/SiO_2 (2, PO_3) catalysts, respectively. The total areas (2.05 and 3.86) fit well with respective H_2/Ni ratios of 2.25 and four derived from the following stoichiometric reaction equations:

$$NiO + 1/2\,(NH_4)_2HPO_4 + 9/4H_2 \rightarrow 1/2\ Ni_2P + NH_3 + 3H_2O \quad (5)$$

$$NiO + 2H_3PO_3 + 4H_2 \rightarrow 1/2\,Ni_2P + 3/8\,P_4 + 7H_2O \quad (6)$$

During reduction of NiO/SiO_2 (2, PO_4) (cf. Equation 5), phosphate is only partially reduced to Ni_2P, whereas all phosphite is reduced to Ni_2P and elemental phosphorus in the case of NiO/SiO_2 (2, PO_3) catalyst (cf. Equation 6).

An alternative approach to obtain Ni_2P is to use phosphite and hypophosphite precursors at high initial P/Ni ratios, followed by activation in a nitrogen flow instead of hydrogen in the 200–250 °C [37, 38]. We prepared similar precursors, i.e. NiO/SiO_2 (6, PO_3) and NiO/SiO_2 (2, PO_2), but neither reduction in H_2 nor activation in N_2 as suggested by literature resulted in Ni_2P. Therefore, we used reduction at 400 °C in hydrogen to ensure proper activation of the precursor.

The XRD patterns of reduced NiO/SiO_2 (2, PO_4), NiO/SiO_2 (2, PO_3) and NiO/SiO_2 (2, PO_2) show phase-pure features of Ni_2P. As the reduced NiO/SiO_2 (6, PO_3) did not show these characteristic features (Fig. 2), we did not include this catalyst in our further studies. Reduced NiO/SiO_2 (2, PO_4) and NiO/SiO_2 (2, PO_3) retained the favorable textural properties of silica. Their Ni and P loadings, pore volumes and BET surface areas were in the same range (Table 2), suggesting that the active phase dispersions of Ni_2P should be not too different in the reduced catalysts. On contrary, low surface area (12 m^2/g) and pore volume 0.07 cm^3/g were observed for reduced NiO/SiO_2 (2, PO_2), indicating that the pores of this catalyst became blocked (Table 2). Elemental analysis (Table 2) shows that the latter catalyst contains a much higher amount of P than that expected for Ni_2P, suggesting that not all PO_2^{3-} was reduced. Thus, it is likely that these species block the pores of the support.

We also derived a catalyst from NiO/SiO_2 prepared by a sol–gel procedure and phosphite impregnation (P/Ni = 2) followed by reduction in hydrogen [30]. XRD shows that the fresh NiO/SiO_2-SG and reduced NiO/SiO_2-SG (2, PO_3) catalysts contained NiO and Ni_2P phases, respectively (Fig. 3). The surface areas of the oxidic and reduced forms were 459 and 73 m^2/g, respectively (Table 2). The surface area of the reduced catalyst was lower than reported in literature [30], likely due to the lower reduction temperature used in the present study leaving a larger amount of P

Table 2 Textural properties and elemental composition of selected silica-supported reduced Ni-phosphide catalysts

Catalyst	S_{BET} (m^2/g)	Pore volume (cm^3/g)	d_{pore} (nm)	Ni (wt%)	P (wt%)	P/Ni
NiO/SiO_2 (2, PO_4)	107	0.69	25.9	6.6	5.5	1.57
NiO/SiO_2 (2, PO_3)	144	0.80	22.2	7.4	5.8	1.48
NiO/SiO_2 (2, PO_2)	12.5	0.07	23.6	7.5	6.2	1.57
NiO/SiO_2-SG	459	0.63	5.5	16.0	–	–
NiO/SiO_2-SG (2, PO_3)	73	0.32	16.9	14.4	18.3	2.42
NiO/SiO_2 (1, PO_4)	140	0.88	22.6	9.9	3.9	0.75

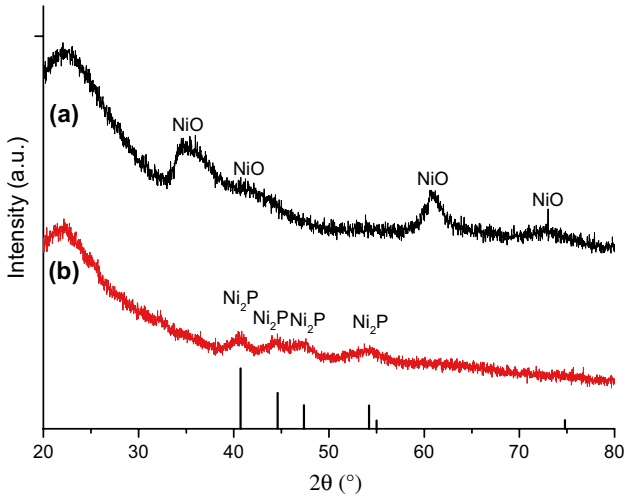

Fig. 3 XRD patterns of *a* NiO/SiO_2-SG and *b* NiO/SiO_2-SG (2, PO_3) catalysts. *Reference lines* of Ni_2P are marked at the *bottom*

unreduced. We argue in the present study that reduction at 540 °C is appropriate for the phosphite-based catalysts.

We then used these catalysts together with $CuMgAlO_x$ in a one pot approach for the upgrading of soda lignin with the purpose to increase the HDO degree. We first discuss three types of reference experiments for comparison, which involved the use of (ref. 1) the $CuMgAlO_x$ catalyst, (ref. 2) the reduced NiO/SiO_2 (2, PO_3) catalyst and (ref. 3) a two-step procedure in which the bio-oil obtained by lignin upgrading using $CuMgAlO_x$ was subjected to a HDO step using reduced NiO/SiO_2 (2, PO_3) or NiO/SiO_2 (2, PO_4).

Conversion of lignin using $CuMgAlO_x$ (ref. 1) yielded 27 wt% lignin monomer (Table 3, entry 1). About 29 wt% of the monomers were ring-hydrogenated and about 47 wt% were completely deoxygenated. The yield of ethanol-derived products (not including alkylated lignin products) is 11 wt%. Self-reactions of ethanol are of the Guerbet-type and yield alcohols and esters [8–10]. The dominant reaction product is 1-butanol. As these reactions negatively affect the process economics, the self-condensation of ethanol should be limited.

When reduced NiO/SiO_2 (2, PO_3) was used as the sole catalyst (ref. 2), the lignin monomer yield was only 3 wt% (Table 3, entry 2). The yield of ethanol products was slightly higher (16 wt%) than in the reference case, mainly due to formation of diethylacetal.

In the two-step approach (ref. 3), the bio-oil stemming from lignin upgrading using $CuMgAlO_x$ (lignin monomer yield 16 wt%) was upgraded in the presence of a Ni-phosphide catalyst in 30 bar of hydrogen. Compared to the starting bio-oil, the lignin monomer yield did not significantly change, showing that no further depolymerization took place, in agreement with the result of the Ni-phosphide-only experiment. On the other hand, the product distribution was very different after the HDO step. The HDO degree of the products reached almost 90% (Table 3 entries 3 and 4). We also studied the influence of the gas phase composition for the case that two catalysts were used. In the absence of hydrogen, the lignin monomer yield was 35 wt% (entry 5 in Table 3). The lignin monomer yield increased to 40 wt% (entry 6 in Table 3) when the autoclave was pressurized with hydrogen at 20 bar.

The HDO and HYD degrees increased when the $CuMgAlO_x$ catalyst was used in combination with NiO/SiO_2 (2, PO_4), NiO/SiO_2 (2, PO_3), and NiO/SiO_2 (2, PO_2) (Table 3, entries 6–8). Only in the combination with NiO/SiO_2 (2, PO_4) the lignin monomer yield was significantly higher at 40 wt%. Despite its higher loading (Table 2) and better dispersed Ni_2P phase (Fig. 3), the combination with NiO/SiO_2-SG (2, PO_3) produced only slightly higher lignin monomer yield (32 wt%), yet with a much lower HDO degree (59%) than in the experiment with NiO/SiO_2 (2, PO_3) (Table 3, entries 9 and 7).

3.2 ASA (5/95) and Al_2O_3 Supported Catalysts

We also investigated ASA and alumina supported Ni catalysts. The XRD patterns of reduced ASA and Al_2O_3 supported Ni catalysts are shown in Fig. 4. For the alumina-supported catalysts, no Ni_2P was observed, which is caused by the strong interaction of Al^{3+} species with phosphorus oxides forming $AlPO_4$ [22]. The particular ASA employed in the present study predominantly

Table 3 Product composition of lignin conversion (ethanol solvent, 340 °C, 4 h) over different catalyst systems ('Cu' refers to the $CuMgAlO_x$ catalyst)

Entry	Catalyst	Lignin monomer yield (wt%)					Aromatic HYD degree (wt%)	HDO degree (wt%)	Ethanol-product yield (wt%)
		HC^{-O}	HC^{+O}	Ar^{-O}	Ar^{+O}	Sum			
1	$CuMgAlO_x$	2.8	5.1	9.9	9.3	27	29	47	11
2	NiO/SiO_2 (2, PO_3)	2.7	0.0	0.0	0.6	3	82	82	16
3	NiO/SiO_2 (2, PO_3)*	2.6	0.6	13.4	2.0	19	17	86	15
4	NiO/SiO_2 (2, PO_4)*	7.7	1.2	15.1	1.5	26	35	89	30
5	'Cu'+NiO/SiO_2 (2, PO_4)$^+$	16.5	4.6	10.0	4.2	35	60	75	30
6	'Cu'+NiO/SiO_2 (2, PO_4)	17.7	4.7	10.9	6.3	40	56	72	37
7	'Cu'+NiO/SiO_2 (2, PO_3)	11.4	2.8	8.2	2.3	25	57	79	35
8	'Cu'+NiO/SiO_2 (2, PO_2)	10.0	3.9	9.4	3.5	27	52	72	34
9	'Cu'+NiO/SiO_2-SG (2, PO_3)	14.1	4.0	4.8	9.1	32	57	59	44
10	'Cu'+NiO/ASA (4, PO_3)	8.6	2.3	7.0	5.3	23	47	67	34
11	'Cu'+NiO/ASA (1, PO_3)	7.8	2.2	3.5	6.5	20	50	56	28
12	'Cu'+NiO/SiO_2-SG (1, PO_4)	14.3	2.5	8.8	5.7	31	53	74	41
13	'Cu'+NiO/SiO_2-SG (1, PO_3)	12.4	2.5	5.5	7.2	28	54	65	39
14	'Cu'+Ni/SiO_2 (1, PO_4)	8.2	3.4	5.0	4.8	21	54	62	25
15	'Cu'+Ni/SiO_2 (1, PO_3)	6.0	0.4	7.7	3.6	18	36	78	26
16	'Cu'+NiO/SiO_2 (1, PO_4)	20.5	2.1	23.1	6.8	53	43	83	14

*Two-step approach: feedstock was lignin oil obtained by lignin conversion using $CuMgAlO_x$ catalyst

$^+$Measurement under 20 bar nitrogen pressure

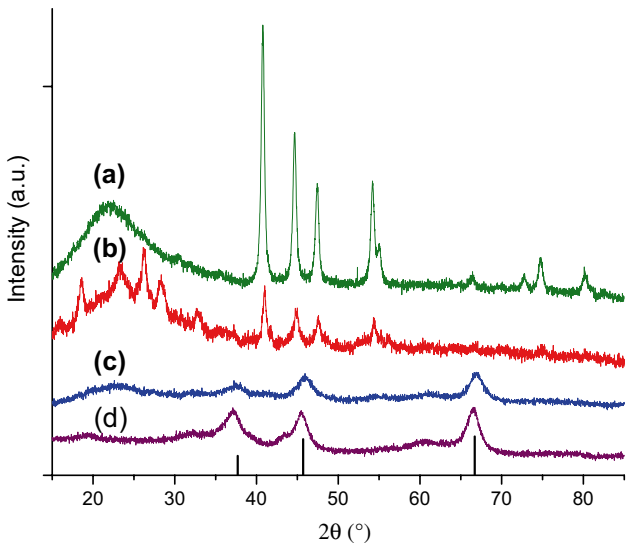

Fig. 4 XRD patterns of *a* NiO/ASA (1, PO_3), *b* NiO/ASA (4, PO_3), *c* NiO/Al_2O_3 (4, PO_3), and *d* NiO/Al_2O_3 (1, PO_2) catalysts. *Reference lines* of Al_2O_3 are marked at the *bottom*

contains relatively strongly bound tetrahedral Al species on a silica surface. At a P/Ni ratio of 1, a relatively pure Ni_2P phase was obtained after reduction at 540 °C [NiO/ASA (1, PO_3)]. At P/Ni = 4, a mixture of Ni_2P with $Al(OH)_3 + SiO_2$ was obtained. Although Ni_2P was obtained on the ASA support, their use in combination with $CuMgAlO_x$ led to lower lignin monomer yields (Table 3, entries 10, 11) in comparison with the $CuMgAlO_x$ reference case. Different from literature [37, 38], the present results for the ASA-supported catalysts (Fig. 4) demonstrate that a high P/Ni precursor ratio is not necessary to obtain phase-pure Ni_2P. Accordingly, we used a P/Ni ratio of 1 in subsequent experiments.

3.3 SiO_2 Supported Catalysts with P/Ni = 1

NiO/SiO_2 and silica-supported co-impregnated catalysts using phosphate and phosphite precursors were also used as co-catalysts for lignin conversion (Table 1, entries 12–15). The sol–gel prepared catalyst was obtained by consecutive impregnation of the P source to the NiO/SiO_2-SG precursor. Hypophosphite was excluded from these experiments in view of the results obtained for these catalysts in lignin upgrading (Table 3, entries 6–8). XRD showed that these catalysts contained phase-pure Ni_2P (Fig. 5). Consecutively impregnated Ni_2P catalysts (NiO/SiO_2) allowed obtaining higher lignin monomer yields than co-impregnated ones (Ni/SiO_2). Nevertheless, these catalysts did not perform better than the combination with the NiO/SiO_2 (2, PO_4) catalyst (Table 3, entry 6). Generally, the PO_4 catalysts gave better results than the PO_3 ones.

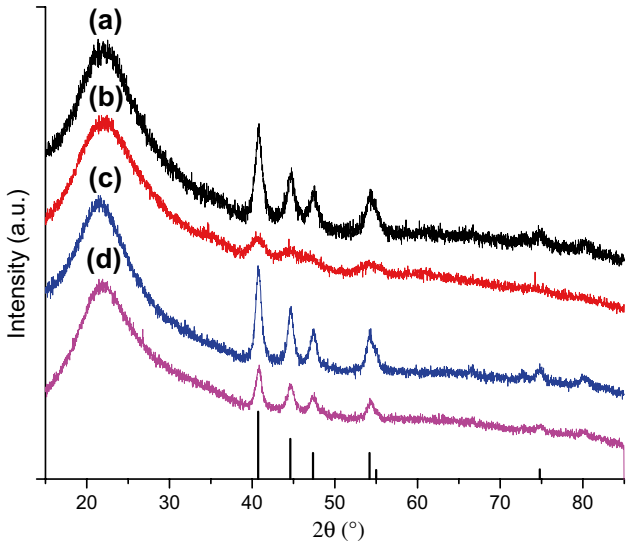

Fig. 5 XRD patterns of *a* NiO/SiO_2-SG (1, PO_4), *b* NiO/SiO_2-SG (1, PO_3), *c* Ni/SiO_2 (1, PO_4), and *d* Ni/SiO_2 (1, PO_3) catalysts. *Reference lines* of Ni_2P are marked at the *bottom*

3.4 Performance of the Optimized Ni_2P/SiO_2 Catalyst

Based on the above results, we conclude that the PO_4 precursor in combination with silica yields the best HDO catalyst in combination with the $CuMgAlO_x$ catalyst used for lignin upgrading. The optimum preparation involves consecutive impregnation of Ni and P, an initial P/Ni ratio of 1 and a reduction temperature of 620 °C. Thus obtained Ni_2P/SiO_2—NiO/SiO_2 (1, PO_4)—has a surface area of 140 m^2/g and a much lower final P/Ni ratio (0.75) than the other catalysts (Table 2). This shows that most of the phosphate in the precursor has been reduced, making the active Ni_2P accessible for catalysis. In the conversion of soda lignin (Table 3, entry 16), this catalyst showed clear synergy with the $CuMgAlO_x$ catalyst, presenting the highest lignin monomer yield (53 wt%) and HDO degree (83 wt%). The aromatic HYD level was only 43 wt% in this case. The optimized two-catalyst system presented very promising performance in comparison to other Ni-based catalyst systems used for bio-oil and lignin upgrading [27, 28].

We discussed and explained the synergistic and cooperative activation of this optimized two-catalysts system in terms of monomeric product yield and HDO selectivity in more detail in a recent paper [39]. Briefly, the synergy relates to the in situ production of hydrogen by the $CuMgAlO_x$ component, maintaining the Ni_2P surface in its active state. The Ni_2P catalyst contributes to removing oxygen functionalities from released monomers, thereby reducing the propensity to condensation and, overall, increasing the HDO selectivity. The solid product/catalysts mixtures are very complex. Extracting the catalysts from it would involve treatment with strong acids which would at least partly oxidize the metal phosphides. Therefore, we did not attempt to extract and analyse the spent catalyst from the solids.

4 Conclusions

Preparation of phase-pure Ni_2P can be achieved on silica and siliceous amorphous silica-alumina. The preferred preparation involves a low initial P/Ni precursor, phosphate as P-source and a relatively high reduction temperature of 620 °C. When free aluminium species are present as in g-alumina, Ni_2P cannot be obtained. Although the use of phosphite and hypophosphite can also render Ni_2P on silica at lower reduction temperature, residual P-oxides block the pores and limit the surface area of the catalyst. Ni_2P catalysts displayed very little activity in lignin depolymerization. Conversion of a lignin oil derived from depolymerization of soda lignin in ethanol using $CuMgAlO_x$ demonstrated that Ni_2P/SiO_2 is an active catalyst for the HDO of lignin monomers. The HDO degree increased from 47 to 86 wt%. Combining $CuMgAlO_x$ and Ni_2P/SiO_2 proved synergistic in the one-step upgrading of lignin in ethanol at 340 °C, achieving more than 50 wt% lignin monomers at a HDO degree of >80 wt%.

References

1. Zakzeski Z, Bruijnincx PCA, Jongerius AL, Weckhuysen BM (2010) The catalytic valorization of lignin for the production of renewable chemicals. Chem Rev 110:3552–3599. doi:10.1021/cr900354u
2. Behling R, Valange S, Chatel G (2016) Heterogeneous catalytic oxidation for lignin valorization into valuable chemicals: what results? What limitations? What trends?. Green Chem 18:1839–1854. doi:10.1039/c5gc03061g
3. Strassberger Z, Tanase S, Rothenberg G (2014) The pros and cons of lignin valorisation in an integrated biorefinery. RSC Adv 4:25310–25318. doi:10.1039/c4ra04747h
4. Peretti SW, Barton R, Mendonca RT. Lignin as feedstock for fibers and chemicals (2016) In: Snyder SW (ed) RSC Green

Chemistry Series 43 (commercializing biobased products). RSC, London, p 132–165. doi:10.1039/9781782622444-00132.
5. Rinaldi R, Jastrzebski R, Clough MT, Ralph J, Kennema M, Bruijnincx PCA, Weckhuysen BM (2016) Paving the way for lignin valorisation: recent advances in bioengineering, biorefining and catalysis. Angew Chem Int Ed 55:8164–8215. doi:10.1002/anie.201510351
6. Xie S, Ragauskas AJ, Yuan JS (2016) Lignin conversion: opportunities and challenges for the integrated biorefinery. Ind Biotechnol 12:161–167. doi:10.1089/ind.2016.0007
7. Li C, Zhao X, Wang A, Huber GW, Zhang T (2015) Catalytic transformation of lignin for the production of chemicals and fuels. Chem Rev 115:11559–11624. doi:10.1021/acs.chemrev.5b00155
8. Huang X, Korányi TI, Boot MD, Hensen EJM (2014) Catalytic depolymerization of lignin in supercritical ethanol. ChemSusChem 7:2276–2288. doi:10.1002/cssc.201402094
9. Huang X, Korányi TI, Boot MD, Hensen EJM (2015) Ethanol as capping agent and formaldehyde scavenger for efficient depolymerization of lignin to aromatics. Green Chem 17:4941–4950. doi:10.1039/c5gc01120e
10. Huang X, Atay C, Korányi TI, Boot MD, Hensen EJM (2015) Role of Cu–Mg–Al mixed oxide catalysts in lignin depolymerization in supercritical ethanol. ACS Catal 5:7359–7370. doi:10.1021/acscatal.5b02230
11. Loehre C, Barth T, Kleinert M (2016) The effect of solvent and input material pretreatment on product yield and composition of bio-oils from lignin solvolysis. J Anal Appl Pyrolysis 119:208–216. doi:10.1016/j.jaap.2016.03.003
12. Güvenatam B, Heeres HJ, Pidko EA, Hensen EJM (2016) Lewis acid-catalyzed depolymerization of soda lignin in supercritical ethanol/water mixtures. Catal Today 269:9–20. doi:10.1016/j.cattod.2015.08.039
13. Barta K, Matson TD, Fettig ML, Scott SL, Iretskii AV, Ford PC (2010) Catalytic disassembly of an organosolv lignin via hydrogen transfer from supercritical methanol. Green Chem 12:1640–1647. doi:10.1039/c0gc00181c
14. Barta K, Ford PC (2014) Catalytic conversion of nonfood woody biomass solids to organic liquids. Acc Chem Res 47:1503–1512. doi:10.1021/ar4002894
15. Deuss PJ, Barta K (2016) From models to lignin: transition metal catalysis for selective bond cleavage reactions. Coord Chem Rev 306:510–532. doi:10.1016/j.ccr.2015.02.004
16. Cheng SN, D'cruz I, Wang MC, Leitch M, Xu CB (2010) Highly efficient liquefaction of woody biomass in hot-compressed alcohol-water co-solvents. Energy Fuels 24:4659–4667. doi:10.1021/ef901218w
17. Matson TD, Barta K, Iretskii AV, Ford PC (2011) One-pot catalytic conversion of cellulose and of woody biomass solids to liquid fuels. J Am Chem Soc 133:14090–14097. doi:10.1021/ja205436c
18. Maxwell IE, Naber JE, de Jong KP (1994) The pivotal role of catalysis in energy related environmental technology. Appl Catal A 113:153–173. doi:10.1016/0926-860X(94)80024-3
19. Miller JE, Evans L, Littlewolf A, Trudell DE (1999) Batch microreactor studies of lignin and lignin model compound depolymerization by bases in alcohol solvents. Fuel 78:1363–1366. doi:10.1016/S0016-2361(99)00072-1
20. Ma R, Hao WY, Ma XL, Tian Y, Li YD (2014) Catalytic ethanolysis of kraft lignin into high-value small-molecular chemicals over a nanostructured α-molybdenum carbide catalyst. Angew Chem Int Ed 53:7310–7315. doi:10.1002/anie.201402752
21. Boullosa-Eiras S, Lødeng R, Bergem H, Stöcker M, Hannevold L, Blekkan EA (2014) Chapter 2: potential for metal-carbide, -nitride, and -phosphide as future hydrotreating (HT) catalysts for processing of bio-oils. In Spivey J, Dooley KM, Han YF (ed) Catalysis, Vol. 26. RSC, London, p 29–71. doi:10.1039/9781782620037-00029.
22. Prins R, Bussell ME (2012) Metal phosphides: preparation, characterization and catalytic reactivity. Catal Lett 142:1413–1436. doi:10.1007/s10562-012-0929-7
23. Lee YK, Oyama ST (2006) Comparison of structural properties of SiO_2, Al_20_3, and C/Al_20_3 supported Ni_2P catalysts. Stud Surf Sci Catal 159:357–360. doi:10.1016/S0167-2991(06)81607-1
24. Cho KS, Seo HR, Lee YK (2011) A new synthesis of highly active Ni_2P/Al_2O_3 catalyst by liquid phase phosphidation for deep hydrodesulfurization. Catal Commun 12:470–474. doi:10.1016/j.catcom.2010.10.016
25. Sawhill SJ, Phillips DC, Bussell ME (2003) Thiophene hydrodesulfurization over supported nickel phosphide catalysts. J Catal 215:208–219. doi:10.1016/S0021-9517(03)00018-6
26. Shu Y, Lee YK, Oyama ST (2005) Structure-sensitivity of hydrodesulfurization of 4,6-dimethyldibenzothiophene over silica-supported nickel phosphide catalysts. J Catal 236:112–121. doi:10.1016/j.jcat.2005.08.015
27. Koike N, Hosokai S, Takagaki A, Nishimura S, Kikuchi R, Ebitani K, Suzuki Y, Oyama ST (2016) Upgrading of pyrolysis bio-oil using nickel phosphide catalysts. J Catal 333:115–126. doi:10.1016/j.jcat.2015.10.022
28. Kasakov S, Shi H, Camaioni DM, Zhao C, Baráth E, Jentys A, Lercher JA (2015) Reductive deconstruction of organosolv lignin catalyzed by zeolite supported nickel nanoparticles. Green Chem 17:5079–5090. doi:10.1039/c5gc02160j
29. Hensen EJM, Poduval DG, Magusin PCMM, Coumans AE, van Veen JAR (2010) Formation of acid sites in amorphous silica-alumina. J Catal 269:201–218. doi:10.1016/j.jcat.2009.11.008
30. Chen J, Chen Y, Yang Q, Li K, Yao CC (2010) An approach to preparing highly dispersed Ni_2P/SiO_2 catalyst. Catal Commun 11:571–575. doi:10.1016/j.catcom.2009.12.022
31. Grob RL, Barry EF (2004) Modern practice of gas chromatography. Wiley, Hoboken, p 302–303. ISBN 0-471-22983-0.
32. Korányi TI, Vít Z, Poduval DG, Ryoo R, Kim HS, Hensen EJM (2008) SBA-15-supported nickel phosphide hydrotreating catalysts. J Catal 253:119–131. doi:10.1016/j.jcat.2007.10.012
33. Zhao HY, Li D, Bui P, Oyama ST (2011) Hydrodeoxygenation of guaiacol as model compound for pyrolysis oil on transition metal phosphide hydroprocessing catalysts. Appl Catal A 391:305–310. doi:10.1016/j.apcata.2010.07.039
34. Oyama ST, Wang X, Lee YK, Bando K, Requejo FG (2002) Effect of phosphorus content in nickel phosphide catalysts studied by XAFS and other techniques. J Catal 210:207–217. doi:10.1006/jcat.2002.3681
35. Rodriguez JA, Kim JY, Hanson JC, Sawhill SJ, Bussell ME (2003) Physical and chemical properties of MoP, Ni_2P, and MoNiP hydrodesulfurization catalysts: time-resolved X-ray diffraction, density functional, and hydrodesulfurization activity studies. J Phys Chem B 107:6276–6285. doi:10.1021/jp022639q
36. Cecilia JA, Infantes-Molina A, Rodrıguez-Castellon E, Jimenez-Lopez A (2009) The influence of the support on the formation of Ni_2P based catalysts by a new synthetic approach. Study of the catalytic activity in the hydrodesulfurization of dibenzothiophene. J Phys Chem C 113:17032–17044. doi:10.1021/jp904263c
37. Song L, Zhang S, Wei Q (2011) A new route for synthesizing nickel phosphide catalysts with high hydrodesulfurization activity based on sodium dihydrogenphosphite. Catal Commun 12:1157–1160. doi:10.1016/j.catcom.2011.03.038

38. Shi G, Shen J (2009) Mesoporous carbon supported nickel phosphide catalysts prepared by solid phase reaction. Catal Commun 10:1693–1696. doi:10.1016/j.catcom.2009.05.009
39. Korányi TI, Huang X, Coumans AE, Hensen EJM (2017) Synergy in lignin upgrading by a combination of Cu-based mixed oxide and Ni-phosphide catalysts in supercritical ethanol. ACS Sustain Chem Eng 5(4):3535. doi:10.1021/acssuschemeng.7b00239 (**in press**)